AD-A062 604 OHIO STATE UNIV RESEARCH FOUNDATION COLUMBUS F/G 11/6
SURFACE ENERGIES AND RELATED PROPERTIES OF BETA-TITANIUM ALLOYS--ETC(U)
NOV 78 G MEYRICK, R SPEISER AFOSR-75-2799

UNCLASSIFIED OSURF/760216/784090 AFOSR-TR-78-1520 NL

| OF |
ADA
062604

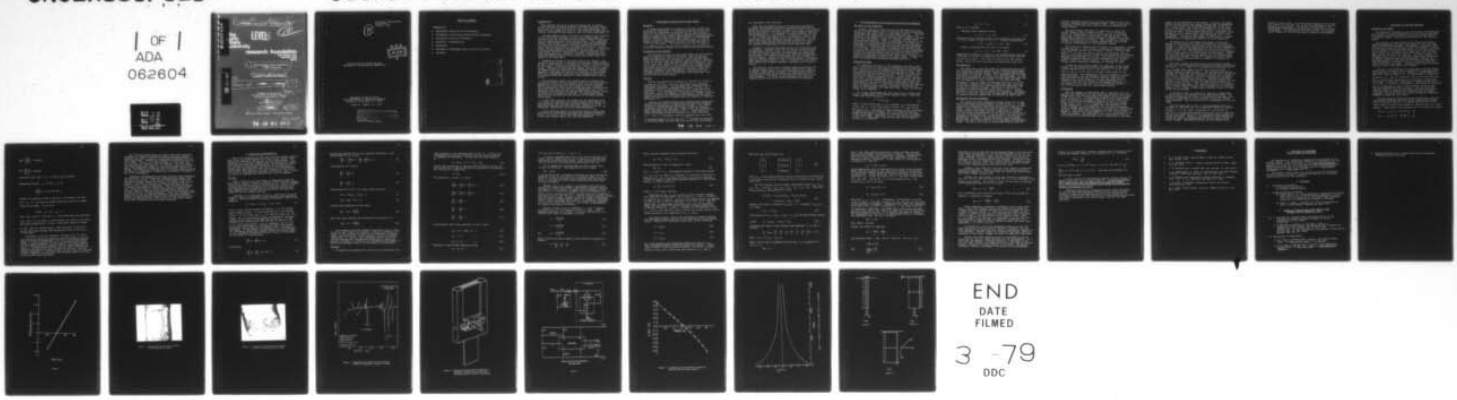

END
DATE
FILMED
3 -79
DDC

(18) AFOSR (19) TR-78-1520 (14) OSURF RF Project 760216/784090
Final Report

(10)

LEVEL II

the ohio state university

research foundation

1314 kinnear road
columbus, ohio
43212

(6) SURFACE ENERGIES AND RELATED PROPERTIES OF Beta TITANIUM ALLOYS.

(10) Glyn Meyrick and Rudolph Speiser
Department of Metallurgical Engineering

(9) Final rept. 1 Jan 75 - 31 Aug 78

DEPARTMENT OF THE AIR FORCE
Air Force Office of Scientific Research
Bolling Air Force Base, D.C. 20332

(15) Grant No AFOSR-75-2799

(11) 1 Nov 78 (12) 34 p.

Approved for public release; distribution unlimited

267360

RF Project 760216/784090
Final Report
October , 1978

(10)

Glyn Meyrick and Rudolph Speiser
Department of Metallurgical Engineering

Department of the Air Force
Air Force Office of Scientific Research
Bolling Air Force Base, D.C. 20332

Grant No. AFOSR - 75 - 2799

TABLE OF CONTENTS

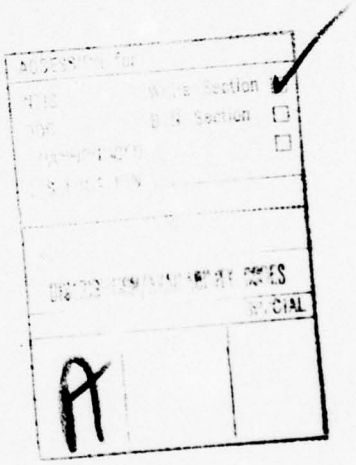

Introduction

The original aim of this research program was to measure surface and grain boundary energies in B-titanium alloys; namely Ti-Mo and Ti-V in the pure state and also when containing trace amounts of the elements of group B. The technical reasons for such an investigation have been set forth in detail previously.(1)

The experimental method available to accomplish this objective was the zero-creep technique, in which the surface energy is evaluated from the load that exactly prevents creep in fine wires held at temperatures near their melting points. This technique requires the specimens to be maintained at the high temperatures for many hours which presents a serious problem in view of the great chemical reactivities of the materials involved. Accordingly, the investigation was approached in two ways. In the first, a sophisticated apparatus comprising a furnace within an ultra-high vacuum system was constructed in which conventional zero-creep experiments were conducted. Secondly, research was initiated into modifications of the technique that would reduce the length of the experiments.

Vanadium was chosen as the first metal to be studied. This choice was made because it undergoes no allotropic transformation as does titanium and has a melting point (1890°C) similar to those of the alloys. Furthermore vanadium can dissolve up to 3.5 wt% of oxygen. Therefore by enclosing the samples within several grams of vanadium foil and conducting the experiments within a sealed apparatus containing very low partial pressures of active gases, there was a reasonable probability that meaningful data could be obtained before the formation of bulk surface phases such as oxides.

The preliminary results were promising but as events transpired the surface energy of vanadium could not be satisfactorily determined by the zero-creep method within the time allotted. However, the second phase of the program was very successful. This investigation, which began by exploring means of sensitively measuring creep rates in-situ and at temperature, led to the invention of a new method for determining surface energies called the strain-load relaxation technique. The associated instrumentation was developed and the validity of the method proven using copper.

In the final analysis, the creation of the technique which will permit the evaluation of surface energies more rapidly and more accurately than has been previously possible is a more significant advance than would have been achieved merely by the successful completion of the zero-creep experiments.

In the following report the principal features of the work performed will be described including some theoretical developments. For brevity, parts that have been presented in detail in previous interim reports will only be summarized.

A. Experiments Using The Zero-Creep Method

Apparatus

A unique high-temperature vacuum or inert gas furnace was designed and constructed. A detailed description of this apparatus and its performance is presented in the first interim report.[1] The furnace, comprising a tungsten mesh heating element surrounded by an array of refractory metal radiation shields mounted within a water-cooled copper chamber, is incorporated within a stainless steel ultra-high vacuum system. It was designed to attain a temperature of 2400°C and has been used at 1750°C for many hours. This temperature has been attained in in a vacuum of 10^{-8} torr and also in argon which was admitted to the pre-evacuated chamber via an external purification system.

Experiments with Vanadium

The procedure followed in these experiments was that usually used in conventional zero-creep studies. Gage-lengths were marked on samples of 0.005 in. wire of 99.95% pure vanadium which had been previously cleaned and vacuum-annealed. Weights, chosen to be both larger and smaller than that which would yield a zero creep-rate, were made from vanadium and attached to the lower ends of the samples. The specimens were suspended within the furnace and held at temperature for 25 hours, after which they were removed and the gage-lengths measured by means of a Gaertner micrometer slide cathetometer. Repetition of this procedure until the rates of creep have been established constitutes the zero-creep method.

Results

Because the apparatus was capable of operation at 1700°C in a vacuum of 10^{-8} torr, the first experiments were attempted under these conditions. The specimens were suspended within a cylindrical enclosure of vanadium sheet which, in turn, was contained within a closed tungsten crucible lined with molybdenum foil. This arrangement proved to be insufficient to prevent early loss of the samples by evaporation. Because a massive vanadium enclosure was unavailable the remainder of the experiments were carried out in argon which was purified as described previously.[1]

Progress was hindered because the vanadium wires became very fragile and were prone to break during the handling procedures involved in determining the dimensional changes. For a while no samples survived beyond fifty hours so that the measured creep rates were very unreliable. Some of the data obtained in these experiments are presented in Fig. 1. These results indicate the surface energy of vanadium to be about 2000 ergs cm^{-2}. This is a reasonable value and compares quite well with a calculated figure of 1950 ergs cm^{-2}.[2] Although the precision of the measurements was very poor the results were encouraging

and experiments were continued.

After various modifications of the detailed experimental procedure the frequency with which specimens fractured was reduced and individual lifetimes in excess of 100 hrs. were achieved. During this phase of the work a surface scale began to appear on the vanadium wires. It originated at grain boundaries and then spread gradually over the surface. An example is shown in Fig. 2. Fig. 3 shows the surface of an intergranular fracture indicating that the phase formed on the grain boundaries. The formation and growth of this phase probably accounts for much of the erratic creep behavior observed and because the results are considered unsatisfactory they are not presented here.

Attempts to identify the phase using X-ray diffraction were inconclusive. Because of the very low oxygen partial pressure in equilibrium with the oxide, it was natural to suspect that filling the closed system with purified argon and surrounding the specimens with vanadium sheet might have been inadequate to avoid oxidation. However the surface phase was insoluble in chemical reagents capable of dissolving the oxides. Furthermore auger spectroscopic analysis, Fig. 4, revealed a strong carbon peak whereas the vanadium originally contained only 55 ppm of carbon.

The identity of the phase concerned remains uncertain, but it appears likely that it is a carbide rather than an oxide. No obvious single source of carbon contamination was found and it became clear that the elimination of contamination would require major modifications to the apparatus and would be very time-consuming. For these reasons titanium alloys were not examined and the use of the zero-creep method was abandoned.

B. The Development of The Strain-Load Relaxation Technique

The Birth of the Technique

Initially the aim of this part of the investigation was to improve the experimental means of applying the zero-creep method. Accordingly ways were sought to continuously monitor the creep rates while the samples were actually undergoing creep. One approach, that appeared to be promising, was to impose a constant stress upon the sample by means of a remotely located lever-arm and fulcrum balance. Then, by recording the rotation of the lever-arm the creep rate would be established. The major disadvantage of this approach was that it would require successive experiments at different loads to establish that corresponding to zero-creep. While methods of measuring the rotation of the lever-arm were being developed, the presence of this disadvantage so haunted the investigators that its exorcism became manditory. Finally the idea was conceived of replacing the fulcrum by a tension wire suspension system which would produce a stress that would be automatically varied as the sample crept. At this point the strain-load relaxation technique was born.

Theoretical Basis

To appreciate the basis of this technique, consider a specimen, in the form of a thin foil, suspended within a furnace in such a way that it can be subjected to a tensile stress by means of a tungsten torsion wire situated outside the hot zone. The magnitude of the stress exerted on the specimen is proportional to the twist-angle of the torsion wire. If this angle is set initially to provide a tensile stress in excess of the contractile stress in the specimen due to its surface energy, the specimen will extend by diffusional creep. When creep occurs, the twist-angle of the torsion wire will decrease and so will the applied tensile stress. In principle, this process will continue until the applied stress exactly counteracts the contractile stress in the specimen, and creep will cease. Thus, the surface energy can be computed.

It is well established that the strain-rate in diffusional creep is proportional to the excess applied stress. Thus, the strain rate can be written as

$$\dot{\varepsilon} = k\,(\sigma_a - \sigma_o), \qquad (1)$$

where ε is the strain rate, k is a constant, σ_a is the applied stress, and σ_o is the "zero-creep" stress; i.e., that stress for which $\dot{\varepsilon} = 0$. For amall strains the change in the twist-angle is proportional to the strain. Also, for a torsion wire the change in the stress it produces is proportional to the change in the twist-angle. Therefore, if σ_1 is the initial stress and a strain of ε takes place, then the new value of the applied stress, σ_a, is given by

$$\sigma_a = \sigma_1 - m\,\varepsilon, \tag{2}$$

where m is a constant.

Combining these equations yields

$$\dot{\varepsilon} = k\,(\sigma_1 - \sigma_o - m_\varepsilon). \tag{3}$$

Integrating this equation subject to the boundary conditions that $\varepsilon = 0$ at t (time) = 0 and $\dot{\varepsilon} = 0$ at $t \to \infty$ yields the expression

$$\varepsilon = [(\sigma_1 - \sigma_o)/m]\ \{1 - \exp - kmt\}. \tag{4}$$

Finally, from equations (2) and (4) we obtain

$$\sigma_a = \sigma_o + (\sigma_1 - \sigma_o)\ (\exp - kmt). \tag{5}$$

Comparison of equations (4) and (5) with experimentally measured variations of σ_a and ε as functions of time will permit the calculation of σ_o and k. The former of these yields the surface energy, while the latter describes the diffusional creep rate.

The Apparatus

The search for a practical means of accomplishing the strain-load relaxation technique ended with the successful development of a capacitance-tension balance capable of simultaneously measuring small stresses and strains. As is generally true the final instrument was preceded by others that were discarded. In this case an interferometric strain gage was developed that might well have applications in other research. It has been described previously[1] and is capable of measuring rotations of 10^{-5} rad. In essence a collimated light beam is reflected from a rotating mirror into a Fabry-Perot interferometer which generates a set of moving interference fringes. The shift of the fringes is detected by a photo transistor whose output is fed to a chart recorder so that the rate of rotation is continuously monitored. While this system was successful the capacitance-tension balance is superior and more compact and is described in detail here .

Description of the Instrument

The torsion wire and capacitance system, which will be termed the capacitance-torsion balance, is shown in Fig. 5. A tungsten wire is supported horizontally and in tension with its ends clamped within stainless steel slugs attached to a Duralumin frame. Fixed to the central portion of the wire is a vertical stainless-steel plate which carries a symmetrically located lever arm mutually perpendicular to the plane of the plate and to the axis of the torsion wire. From one end of the lever arm is suspended the linkage to the specimen which, in the present application, is within a furnace vertically below the balance. On the other end of the lever-arm is an adjustable counterbalance weight. One half of the plate is positioned between a pair of

parallel condenser plates that are firmly attached to, but electrically insulated from the Duralumin frame. These plates can be conveniently fabricated from copper-coated resin-bonded glass circuit boards.

The three plates constitute two capacitors in which the central movable plate is common to each. As the torsion wire twists, the capacitance of one of the capacitors is increased while that of the other is decreased by the same amount. The capacitance changes are directly related to changes in the angle through which the wire is twisted. These changes are linearly related to variations in the torque imposed upon the wire and to vertical displacements of the suspension linkage.

The electronic circuitry used to monitor the capacitance changes is shown in Fig. 6. This circuit is based on an ingenious diode-quad arrangement devised and described in detail by Harrison and Dimeff.[3] A stable dc supply activates an oscillator that supplies a square-wave input of 0.5 MHz to the diode-quad circuit which generates a dc voltage as an output. This output is monitored by a digital voltmeter and also by an electrometer which, in turn, passes a signal to a chart recorder. In this way the output voltage can be continuously measured as a function of time.

As shown by Harrison and Dimeff the magnitude of the voltage produced by the diode-quad circuit is proportional to the peak voltage impressed upon it and to the ratio $(C_1 - C_2)/(C_1 + C_2)$, where C_1 and C_2 are the pair of variable capacitances on the torsion balance. This demonstrates that an arrangement in which both capacitances vary and change in opposite senses is more sensitive than one in which a single variable capacitance is compared with a fixed reference. A major advantage of this circuit is that with the capacitive arrangement described, output signals of the order of a volt can be obtained directly, thus eliminating any need for signal amplification.

Performance

Both the changes in displacement and in load that are to be measured are transmitted via the suspension linkage to the torsion balance where they are translated into changes in the twist-angle of the torsion wire. Corresponding changes in the capacitances cause variations in the output voltage of the diode-quad circuit. With the capacitance arrangement depicted in Fig. 1 a voltage change from -1.4 to +1.4 V is produced by the maximum movement of the common plate. It is evident that the magnitude of the range of changes in displacement and in stress that correspond to this voltage range are dictated by the geometrical configuration employed. With the present arrangement the full scale voltage change is achieved by a displacement of 2×10^{-2} cm applied to the lever arm linkage. The magnitude of the displacement range can be decreased or increased without loss in sensitivity by suitable

changes in the dimensions of the balance. Similarly the magnitude of the associated load changes depends upon the dimensions of the torsion wire and the mechanical advantage of the lever arm. In particular, the torque corresponding to a given angle of twist is proportional to the fourth power of the radius of the torsion wire. In the present application, variations corresponding to several grams weight were desired for which a wire of diameter 2.5×10^{-2} cm and a lever-arm length of 0.5 cm is appropriate. Alternative load ranges, either smaller or larger are accessible by appropriate selection of these dimensions.

Calibration of the instrument with respect to the load applied to the lever arm is simply performed by recording the voltage as a function of known weights hung from the suspension linkage. In the current application the lever arm and suspension linkage is initially counterbalanced so that the lever arm is tilted upwards, i.e., the torsion wire is twisted in the opposite sense to that caused by the application of the weights. Weights are then added and successively removed from the linkage while the output is measured. During this process and when in actual use the system is enclosed within a chamber to eliminate the effects of drafts.

The output voltage obtained during this procedure changes sign as the rotating plate passes through the symmetrical position for which $c_1 = c_2$. From -0.6 V through the null position to 0.6 V the voltage varies almost linearly with applied weight. A typical example is shown in Fig. 7. The sensitivity of the instrument is essentially the sensitivity with which the voltage can be measured. With the chart recorder in present use voltages in Fig. 7 can be determined to ± 0.0025 V, although the instrument itself is considerably more sensitive. Repeated calibrations carried out at various times on the same torsion balance have all agreed to within 0.003 V. Thus the precision and sensitivity are of similar magnitudes. The long-term stability is excellent. Tests in which constant weights were suspended for 24-h periods showed that the output voltage remains constant within the sensitivity of the recorder.

An important point to recognize is that the voltage range is established by the geometry of the capacitance system. Any geometric change made to select an alternative load-range, such as would be required for a micro-balance, leaves the voltage range unchanged. Thus the sensitivity is independent of the load range.

Over the range used in Fig. 7 the corresponding total displacement of the lower end of the suspended linkage was approximately 5×10^{-3} cm, which corresponds to a sensitivity of $\cong \pm 10^{-5}$ cm. A voltage-displacement calibration curve is identical to the load-voltage curve with the appropriate displacements replacing the loads. However, a displacement-voltage calibration is not so simple an accomplishment as for the case of weight versus voltage. Nevertheless several obvious methods exist

whereby it can be done. In the particular application for which this system is in current use, an absolute knowledge of the displacement is unnecessary. Accordingly the magnitudes of the displacements mentioned were ascertained by means of an optical cathetometer. By changing the electrode spacing the instrument can be adapted for use in even smaller ranges of displacement.

C. Validation of the SLR Technique

Experiments on Copper

For experiments designed to test and develop a new technique it is logical to choose specimens that do not impose additional experimental difficulties and which have already been subject to previous studies. These were the reasons for the choice of copper.

The specimen and capacitance-torsion balance are mounted within an apparatus that could be evacuated to 10^{-7} torr. and then filled with dry hydrogen. The sample is suspended within a quartz tube surrounded by an electric tube furnace. A quartz rod, suspended from a knife-edge support on the lever-arm of the torsion balance is attached to the upper end of the specimen. Rigid copper rods are fixed first to the lower end of the specimen and then to quartz-rod supports. The whole assembly is arranged so that as far as is possible dimensional changes due to thermal expansions are self-compensating. Finally, the apparatus includes a differential screw mechanism that permits fine adjustments to be made, in-situ, to impose any desired initial load upon the sample. Thereafter the variation of that load with time is monitored by the balance.

Analysis of data obtained for copper shows that the experimental curves are indeed closely exponential in agreement with the prediction of equation A.5. However, a single unloading curve (i.e. one for which $\sigma_1 > \sigma$) is insufficient to permit the evaluation of σ_o and the relaxation time mk with good precision. This is because the experiments are restricted to small load excursions. Instead it is necessary to compare two curves for $\sigma_1 > \sigma_o$ and $\sigma_1 > \sigma_o$ where σ_a approaches σ_o from opposite directions. This is illustrated in Fig. 8 where portions of the voltage-time data obtained at 993°C are shown. The two curves are closely similar in form and have been positioned respectively such that they are symmetrically disposed about the common asymptote. The points that are plotted correspond to measured midpoints between the two curves.

The positioning procedure described merely means a lateral displacement along the time axis to the symmetrical position. This is necessary because σ_o is unknown and thus the initial loads cannot be chosen to be greater or smaller than σ_o by equal amounts. Analytically this procedure can be justified as follows:

For $\sigma_1 > \sigma_o$ let $\sigma_1 = \sigma_1^u$ and $\sigma_a = \sigma_a^u$

For $\sigma_1 < \sigma_o$ let $\sigma_1 = \sigma_1^\ell$ and $\sigma_a = \sigma_a^\ell$

Then $\dfrac{\sigma_a^u - \sigma_o}{\sigma_1^u - \sigma_o}$ = exp-mkt

and $\dfrac{\sigma_a^\ell - \sigma_o}{\sigma_1^\ell - \sigma_o}$ = exp=mkt

From which $(\sigma_a^u + \sigma_a^\ell)/2 = \sigma_o + \frac{1}{2}(\sigma_1^u - \sigma_o + \sigma_1^\ell - \sigma_o)$ exp-kmt

Remembering that $\sigma_1^\ell < \sigma_o$, if $\sigma_1^u - \sigma_o = \sigma_o - \sigma_1^\ell$

$$\frac{\sigma_a^u + \sigma_a^\ell}{2} = \sigma_c \text{ for any time t.}$$

Because the required values of σ_1^u and σ_1^ℓ are unknown, the term $(\sigma_1^u - \sigma_o + \sigma^\ell - \sigma_o)$ does not vanish unless the curves are symmetrically positioned. If we write

$$\tfrac{1}{2}(\sigma_1^u - \sigma_o + \sigma_1^\ell - \sigma_o) = E$$

then $(\sigma_a^u + \sigma_a^\ell)/2 = E$ exp-kmt + σ_o. This shows that even when $E \neq 0$, $(\sigma_a^u + \sigma_a^\ell)/2 \to \sigma_o$ at large t, which enables the curves to be easily positioned respectively. In Fig. 9 the points shown are values of $(\sigma_a^u + \sigma_a^\ell)/2$ at various times. Their proximity to the horizontal line drawn through them demonstrates that in this case E is very small.

Obtaining σ_o from the asymptotic voltage in Fig. 8 (since the calibration yields the numerical relation between stress and load) and using the dimensions of the foil, the average surface energy γ can be evaluated from $Mg = \gamma\omega$, neglecting the contribution of grain boundaries for the present. The value obtained is 1.47 J/m^2 which can be compared with the values tabulated in Table 1. The main source of error in this result stems from the precision with which the chart recorder can be read. With the present instrument it is believed that the final error is less than 2% which compares very favorably with the much larger errors that arise in zero-creep experiments.

The foregoing demonstrates that the strain-load relaxation technique is a method of measuring surface and grain boundary energies that offers a number of significant advantages over the zero creep method. Results are obtainable with good precision in short times. In Fig. 8 the time involved is forty hours, but it is clear that much shorter times are adequate. This has important implications with respect to the rate of acquisition of data and of the temperature range over which experiments can be conducted. The sensitivity combined with the in-situ operation allows the effects of temperature, composition, environment and morphology to be investigated.

Subsequent experimentation has been directed toward improving the sensitivity of the system and evaluating those aspects that can give rise to errors. There are two main sources from which extraneous voltage changes can arise in the output of the tension balance. The first is physical building vibrations that can cause relatively rapid oscillations. These have been eliminated by mounting the apparatus appropriately and by electronic damping. The second source is small, uncompensated, dimensional changes caused by temperature oscillations in the furnace and also by slow variations in room temperature. These have assumed greater importance as the instrumental sensitivity has been increased. Effects of room temperature changes have now been eliminated but further development awaits better control of the furnace temperature than is possible with the present equipment.

D. Theoretical Considerations

The S.L.R. technique, as does the zero-creep method, measures that stress which when applied to a foil or wire, exactly counteracts the contractile forces due to the surface energy. Its successful use, therefore, depends upon the existence of a known relationship between the surface energy and the measured stress. This question is considered in detail in this section partly because some objections have been raised in the literature and also because there appears to be some confusion for the case of a foil due to inappropriate references to Poisson's ratio. First the case of a wire and then that of a foil will be examined.

The Wire

When a fine wire of a pure metal is annealed at high temperatures it adopts a "bamboo" structure in which the grain boundaries extend entirely across the cross-section. There is abundant evidence that when diffusional creep occurs wires shrink or extend depending upon the magnitude of an applied tensile force. This suggests the existence of a critical force for which the length of the wire remains constant.

Consider, as is indicated in Fig. 9, a portion of a wire of length ℓ, radius r containing n grain boundaries and supporting a mass M. The total Gibbs free energy at constant P and T of the system is

$$E = 2\pi r\ell\gamma + n\pi r^2\gamma_g + V E_I + Mg\ell \qquad (1)$$

where γ is the average surface free energy, γ_g is the average grain boundary energy, V is the volume and E_I is the internal energy, V is the volume and E_I is the internal energy per unit volume. $Mg\ell$ is the potential energy contributed by the mass M relative to an origin at the upper end of the wire. In this expression the contributions from the ends of the wire (e.g. $2\pi r^2\gamma$) have been omitted. This is reasonable for $\ell >> r$ and in any case experimentally, the ends are always constrained. Furthermore, Mg includes the contribution due to the mass of the sample. In the absence of evaporation for a well-annealed wire undergoing dimensional changes through diffusional creep, it is a reasonable assumption that both V and E_I are constant. If the system is in equilibrium

$$\frac{\partial E}{\partial r} dr + \frac{\partial E}{\partial \ell} d\ell = 0 \qquad (2)$$

Furthermore

$$\frac{\partial V}{\partial r} dr + \frac{\partial V}{\partial \ell} d\ell = dV = 0 \qquad (3)$$

Multiplying equation (3) by the Lagrangian multiplier λ and adding equation (2) yields:

$$\left(\frac{\partial E}{\partial r} + \lambda \frac{\partial V}{\partial r}\right)dr + \left(\lambda\frac{dV}{d\ell} + \frac{\partial E}{\partial \ell}\right)d\ell = 0 \tag{4}$$

From equation (4) we have:

$$\frac{\partial E}{\partial r} + \lambda \frac{\partial V}{\partial r} = 0 \tag{5}$$

$$\frac{\partial E}{\partial \ell} + \lambda \frac{\partial V}{\partial \ell} = 0 \tag{6}$$

Substituting for E and V into these equations gives

$$2\pi\ell\gamma + 2n\pi r\gamma_g + \lambda 2\pi r\ell = 0 \tag{7}$$

$$2\pi r\gamma + Mg + \gamma\pi r^2 = 0 \tag{8}$$

Solving these equations for Mg yields

$$Mg = -\pi\gamma r + \frac{nr^2\gamma g}{\ell} \tag{9}$$

where the signs indicate the directions of the forces; i.e.

$$Mg = \pi\gamma r - \frac{nr^2\gamma g}{\ell} \tag{10}$$

The foregoing operations indicate that there exists a value of Mg for which ℓ and r are constant. However, an implicit constraint in the treatment is that the wire maintains a constant shape; specifically its sections remains circular and normally cylindrical, i.e. $r \neq f(x)$. This constraint cannot be strictly true but observations indicate that deviations are small and because an average γ is involved, an experimental measurement of Mg for the stationary state is a valid means of determining γ.

The Foil

To examine the situation for a thin foil we shall apply the

same procedure to the specimen shown in Fig. 10. At first the contribution of the grain boundaries will be neglected merely to simplify the discussion. In this case the total energy E, is

$$E = 2w\ell\gamma + 2\ell\, t\gamma + VE_1 + Mg\ell \tag{11}$$

as was done in the case of the wire the contribution of the two ends of the foil is omitted because the specimen is considered to be a portion of a longer foil.

$$V = w\ell t \tag{12}$$

Now equations 2, 3 and 5, 6 become

$$\frac{\partial E}{\partial \ell} d\ell + \frac{\partial E}{\partial \omega} d\omega + \frac{\partial E}{\partial t} dt + o \tag{13}$$

$$\frac{\partial V}{\partial \ell} d\ell + \frac{\partial V}{\partial \omega} d\omega + \frac{\partial V}{\partial t} dt = o \tag{14}$$

$$\frac{\partial E}{\partial \ell} + \gamma \frac{dV}{\partial \ell} = o \tag{15}$$

$$\frac{\partial E}{\partial \omega} + \gamma \frac{dV}{\partial \omega} = o \tag{16}$$

$$\frac{\partial E}{\partial t} + \gamma \frac{\partial V}{\partial t} = o \tag{17}$$

substituting E and V into equations 15 and 17 gives

$$2\omega\gamma + 2t\gamma + Mg + \gamma\, \omega t = o \tag{18}$$

$$2\ell\gamma + \gamma\, \ell t = o \tag{19}$$

$$2\ell\gamma + \gamma\, \omega\ell = o \tag{20}$$

Equations 19 and 20 when combined, become

$$\gamma t - \gamma\omega = o \tag{21}$$

This can only be true if $\gamma = 0$ or $w = t$.

It can be concluded that there is no value of Mg that will render $\ell=\omega=t=o$, unless the foil is of square cross-section and constrained to maintain that shape. Thus variational calculus does not provide a relationship between Mg and γ for $\ell=o$.

Let us impose the restraint that $w=t$ and a square cross-section is maintained. Then equations 18 to 20 yield

$$Mg = \gamma(w+t) \tag{22}$$

It can be noted that, excluding corrections for grain boundaries, equations 22 and 10 show that for a stationary value of ℓ in bodies of circular and square cross-sectional area the required force is the product of the surface energy and half the cross-sectional perimeter.

Whereas, for a foil, there is no tensile stress that will restrain all dimensional changes, experimental evidence supports the suggestion that changes in length can be prevented, at least temporarily. An alternative approach towards determining this stress is due to Fisher and Dunn[4] and has been used by Hondros.[5] The essence of this approach is to consider surface tractions arising from the surface energy. Because a thin foil under no externally imposed stress can spontaneously reduce its length by diffusional creep it can be concluded that there is a longitudinal component of stress that drives the process. This stress is generated by the surface free energy of the foil.

Suppose we have a foil of dimensions ℓ, ω and t oriented as shown in Fig. 11 with respect to axes x, y and z. Then supposing each face to be subject to a stress generated by the surfaces that bound its perimeter, we have:

$$\sigma_x = \frac{-2\gamma\omega - 2\gamma t}{\omega t} \tag{23}$$

$$\sigma y = \frac{-2\gamma\ell - 2\gamma t}{\ell t} \tag{24}$$

and

$$\sigma_z = \frac{-2\gamma\ell - 2\gamma\omega}{\omega\ell} \tag{25}$$

When a tensile force Mg is added in the x-direction equation 23 becomes

$$\sigma_x = \frac{Mg}{\omega t} - \frac{2\gamma}{\omega} - \frac{2\gamma}{t} \tag{26}$$

Fisher and Dunn combined these equations and wrote

$$\dot{\varepsilon}_x \propto (\sigma_x - \tfrac{1}{2}(\sigma_y + \sigma_z)) \tag{27}$$

where putting $\dot{\varepsilon}_x$ = zero in equation 27 yields

$$Mg = \gamma\omega \tag{28}$$

for $t \ll \omega$ and $t \ll \ell$. Subsequently equation 27 has been written $\varepsilon_x \propto (\sigma_x - \nu(\sigma_y + \sigma_z))$ where ν is referred to as Poisson's ratio and is taken as 1/2. It is here that the elastic and plastic responses of the foil appear to have been confused, because it is the elastic strain, α_x, that is given by

$$\alpha_x = \frac{1}{E}(\sigma_x - \nu(\sigma_y + \sigma_z)) \tag{29}$$

where E is the Young's Modulus.

Referring to Fig. 11, for a foil in which no plastic changes take place and for which Mg=o, the stresses σ_x, σ_y and σ_z are given by equations 23, 24 and 25. The foil will suffer elastic strains rates α_x, and α_y, and α_z given by equations of the form of 29. When the temperature is high enough diffusional flow, e.g. Herring-Nabarro creep, can occur under the action of these stresses, giving rise to plastic strains ε_x, ε_y and ε_z. Because the corresponding strain $\dot{\varepsilon}_x$, $\dot{\varepsilon}_y$ and $\dot{\varepsilon}_z$ are small the elastic strains will always possess those values dictated by the nagnitudes of σ_x, σ_y and σ_z.

For small stresses, theory and experimental evidence indicate the diffusional-creep strain rate to be proportional to the applied stress. Therefore the principal strain rates can be written as

$$\dot{\varepsilon}_x = k_{xx}\sigma_x \tag{30}$$

$$\dot{\varepsilon}_y = k_{yy}\sigma_y \tag{31}$$

$$\dot{\varepsilon}_z = k_{zz}\sigma_z \tag{32}$$

For a well-annealed foil undergoing diffusional creep it is a very reasonable assumption that the volume is invariant. Accordingly a strain in the x-direction caused by the stress σ_x causes strains in the y and z-directions and similarly for ε_y and ε_z.

Thus the total strain rates are:

$$\begin{pmatrix} \dot{\varepsilon}_x \\ \dot{\varepsilon}_y \\ \dot{\varepsilon}_z \end{pmatrix} = \begin{pmatrix} k_{xx} k_{xy} k_{xz} \\ k_{yx} k_{yy} k_{yz} \\ k_{zx} k_{zy} k_{zz} \end{pmatrix} \begin{pmatrix} \sigma_x \\ \sigma_y \\ \sigma_z \end{pmatrix} \qquad (33)$$

where k_{xy} is the proportionality constant describing the contribution to the strain rate in the x-direction due to a stress in the y-direction, etc.

For the isotropic case of vacancy diffusional creep, $k_{xx} = k_{yy} = k_{zz} = k_{11}$. Also $k_{xy} = k_{yz} = k_{xz} = k_{zx} = k_{yz} = k_{zy} = k_{12}$. Substituting k_{11} and k_{12} into equation 33 yields

$$\dot{\varepsilon}_x+\dot{\varepsilon}_y+\dot{\varepsilon}_z = (\sigma_x+\sigma_y+\sigma_z)k_{11} + 2k_{12}(\sigma_x+\sigma_y+\sigma_z)$$

$$= (\sigma_x+\sigma_y+\sigma_z)\ (k_{11} + 2k_{12}) \qquad (34)$$

Because the volume is invariant $\dot{\varepsilon}_x+\dot{\varepsilon}_y+\dot{\varepsilon}_z = o$. In general $(\sigma_x+\sigma_y+\sigma_z) \neq o$, hence

$$k_{12} = -\tfrac{1}{2}\ k_{11} \qquad (35)$$

From equation 33 $\dot{\varepsilon}_x = \sigma_x k_{11} + \sigma_y k_{12} + \sigma_z\ k_{12}$ and substituting from (35)

yields $$\dot{\varepsilon}_x = k_{11}(\sigma_x - \tfrac{1}{2}(\sigma_y + \sigma_z)) \qquad (36)$$

Inserting the values of the stresses from equations 23, 24 and 25 we have

$$\dot{\varepsilon}_x = k_{11}\left(-\frac{2\gamma}{t} - \frac{2\gamma}{\omega} - \frac{1}{2}\left\{-\frac{2\gamma}{t} - \frac{2\gamma}{\ell} - \frac{2\gamma}{w} - \frac{2\gamma}{\ell}\right\}\right) \qquad (37)$$

When $t \ll \omega$; $t \ll \ell$ $\dot{\varepsilon}_x = -k_{11}\ \gamma/t$

When a load of Mg is suspended from the foil $\dot{\varepsilon}_x = k_{11}(Mg/wt - \gamma/t)$ for $\dot{\varepsilon}_x = o$,

$$Mg = \gamma\omega$$

This is the final equation obtained by Fisher and Dunn and used with a grain boundary correction term by Hondros. The derivation presented here, which to our knowledge is original, demonstrates that it is correct and that concern over applicable values of Poisson's ration is irrelevant. If only terms in ℓ are neglected in equation 37, then for

$$\dot{\varepsilon}_x = o, \quad Mg = \gamma(w+t)$$

which demonstrates that in keeping with the square cross-sectioned sample and the cylindrical wire, the load is equal to the product of the specific surface energy and half the perimeter of the cross-sectional area. Unlike these two, however, the value of Mg corresponding to $\dot{\varepsilon}_x = o$ does not make $\dot{\varepsilon}_y = \dot{\varepsilon}_z = o$ and thus, itself, must vary with time. Putting $Mg = \gamma\omega$ in the expression for σ_x and evaluating $\dot{\varepsilon}_y$ and $\dot{\varepsilon}_z$ we obtain

$$\dot{\varepsilon}_y = k_{11}(-3/2\ \gamma/t) \tag{40}$$

$$\dot{\varepsilon}_z = k_{11}(3/2\ \gamma/t) \tag{41}$$

Thus when $\dot{\varepsilon}_x = o$, $\dot{\varepsilon}_y = -\dot{\varepsilon}_z$. Furthermore, the magnitude of the decrease in width, in a given increment of time, exceeds the magnitude of the increase in thickness. Consequently the term $\gamma(w+t)$ decreases with time so that in order to maintain $\dot{\varepsilon}_x = o$ the value of Mg must be continually decreased. This means that a zero-creep load does not exist for a foil! This result is consistent with the variational analysis presented earlier. It is therefore necessary to examine the consequences of this effect on experimental efforts to determine the stationary load. For $\dot{\varepsilon}_x = o$ we have

$$Mg = \gamma(w+t)$$

Thus $d(Mg) = \gamma(dw+dt)$.

Because the volume is invariant,

$$dt = -\frac{d\ell.t}{\ell} - \frac{dw.t}{w}$$

and therefore $d(Mg) = \gamma(dw - d\ell.t/\ell - dw.t/w)$. For $t<<\omega$; $t<<\ell$

$$d(Mg) \simeq \gamma dw$$

and

$$\frac{d(Mg)}{Mg} \simeq \frac{dw}{w} \tag{42}$$

From this it can be seen that the percentage change in the true value of Mg during an experiment is of the same magnitude as that of the width. When determining a strain rate for a given load in the zero-creep technique, creep is usually continued until an overall longitudinal strain of several percent has occurred. During this time the width of the foil changes by a similar amount and hence so does the relevant load for $\dot{\varepsilon}_x = o$. This uncertainty is therefore present in the load interpolated from the strain rate data.

Changes in the width of a foil also occur during a strain-load relaxation experiment. However, because of the great sensitivity, dimensional changes are very small with the result that errors from this source become insignificant.

Another fact that appears to have been generally overlooked is that for a wire or foil the value of Mg for $\dot{\varepsilon}_x = o$ is a function of the length of the sample. For example, if none of the terms in equation 37 are neglected, then for $\dot{\varepsilon}_x = o$ we have

$$Mg = \gamma\omega + \gamma t - \frac{2\gamma\omega t}{\ell} \tag{43}$$

For a cylindrical wire when the end terms, $2\pi r^2\gamma$, are included in equation 1, equation 10 becomes

$$Mg = \pi r\gamma - \frac{nr^2\gamma g}{\ell} - \frac{2\pi r^2\gamma}{\ell} \tag{44}$$

These, apparently paradoxial, statements arise because there exists a particular shape of particular dimensions for which the surface energy is a minimum and thus there is no tendency for such a sample to change and Mg = o. With the constraint that the foil always be bounded by three mutually perpendicular faces of specific surface energy γ, the equilibrium form is clearly a cube. With $w = \ell = t$ equation 43 gives Mg - o. Equations 43 and 44 show that for experiments, where the ends are generally constrained, the dimensions of the sample should be chosen to render the final terms negligible, i.e. $\omega >> t$, $\ell >> t$, $\ell >> r$.

An objection to all of the foregoing discussion is that the shape constraint is not practically feasible. Certainly in a foil some rounding of the edges and also surface topographical changes are to be expected. However, except for extremely long times, the consequences of these minor changes are surely of negligible importance.

Because the grain boundaries were not considered during the discussion for the foil, their influence will be examined now. It is clear that the segments of boundary parallel to the length of the foil will exert forces in the same direction as those due to the free surface. Similarly for those parallel to the width. The precise correction requires a knowledge of the grain size and morphology.

However, as an indication, assuming a square array of grains of side d and grain boundary energy γ_b, the condition for $\varepsilon_x = o$ becomes

$$Mg \simeq + \frac{t\gamma_b}{2d} \qquad (45)$$

For $t \simeq 10^{-3}$cms, $d = 5 \times 10^{-2}$ cms, $\omega = 5 \times 10^{-1}$ cms and $\gamma b \tilde{\simeq} \frac{1}{3}\gamma$, $\frac{t\gamma b}{2d} \simeq 3 \times 10^{-3}\gamma$ and $\gamma\omega = 5 \times 10^{-1}\gamma$. Thus the grain boundary correction term is small.

In this section the relationships between surface energies and applied forces have been thoroughly explored. It has been convincingly demonstrated that the measurement of loads that render $\varepsilon_x = o$ for wires or foils provides a valid method of obtaining the surface free energies of solids.

Additional theoretical considerations made during the course of the work described concerned possible roles of grain boundary energies in phase transformations and led to the formulation of a possible criterion for the initiation of discontinuous precipitation. This work is described in an interim report[7] and has also been published.

E. References

1. R. F. Project 4090, Interim Report, Grant No. AFOSR-75-2799, Jan. to Dec. 1975.

2. V. N. Kozhuckov and S. I. Popel, Russian Journal of Phys. Chem., 47, 645, 1973.

3. D. R. Harrison and J. Dimeff, Rev. Sci Instrum. 44. 1468 (1973).

4. J. C. Fisher and C. G. Dunn, in "Imperfections in Nearly Perfect Crystals", John Wiley and Sons, N.Y., p. 317, 1952.

5. E. D. Hondros, in "Techniques of Metals Research", R. Bunshah (ed.), Vol. IV (A), John Wiley and Sons, N.Y. 1970.

6. L. E. Murr, "Interfacial Phenomena in Metals and Alloys", Addison Wesley, 1975.

7. R. F. 4090, Interim Report, Grant No. AFOSR-75-2799 Jan. 1976-Dec. 1976.

F. Relevance to Long-Range Goals of the U.S. Air Force

The importance of interfacial energies has been pointed out in previous reports. The capacitance transducer in combination with the torsion balance, which is the heart of the Strain-Load Relaxation apparatus, is novel and can be employed not only for measuring interfacial energies but also as an extremely sensitive micro-balance, dilatometer, and a micro-creep apparatus.

The authors of this report are consulting with The Ohio State University Patent Attorney to ascertain the feasibility of making a patent application for the transducer.

G. Personnel

1. Principal Investigators
   (a) Professor Glyn Meyrick
   (b) Professor Rudolph Speiser

2. Graduate Research Assistants
   (a) Dennis Werth. Mr. Werth successfully completed his research and earned an M.Sc. in Metallurgical Engineering, January, 1978. He is now employed in the General Motors Research Laboratory as a Metallurgical Engineer in Michigan.

   (b) Robert T. Werber, completed his research and earned an M.Sc. in Metallurgical Engineering, March 1978.

H. Summary of Publications Under AFOSR-75-2799 October, 1976 to August 31, 1978

(a) 1. Glyn Meyrick, Rudolph Speiser and Dennis Werth, "A New Technique for Measuring Surface Energies of Solids," Scripta Met. 12, 91, (1978).

2. G. Meyrick, R. Speiser, R. Turk and D. Werth, "A Capacitance-Torsion Balance for Measuring Small Stresses and Strains," Rev. Sci. Instrum. 49 (6), 806 (1978).
Glyn Meyrick, "On the Initiation of Discontinuous Precipitation," Scripta. Met. 10, 649, (1976)

(b) Manuscripts in Preparation:

1. R.A. Turk, G. Meyrick and R. Speiser, "An Optical Strain Gauge: for Rev. of Sci. Instr. or J. Opt. Soc.

2. R. A. Turk, G. Meyrick and R. Speiser, "High Temperature Vacuum Furnace for Rev. Sci. Instr. or High Temperature Chemistry.

(c) Patent application for a "Capacitance-Torsion Transducer." (Economics being considered!)

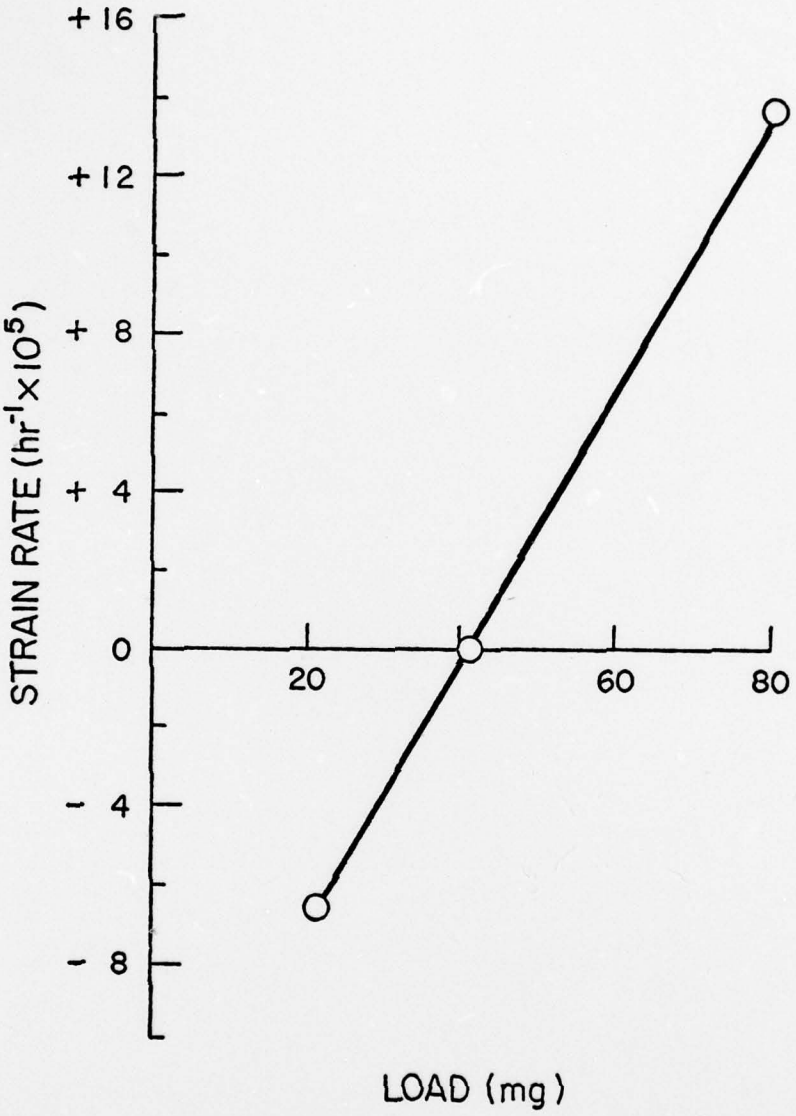

Figure 1

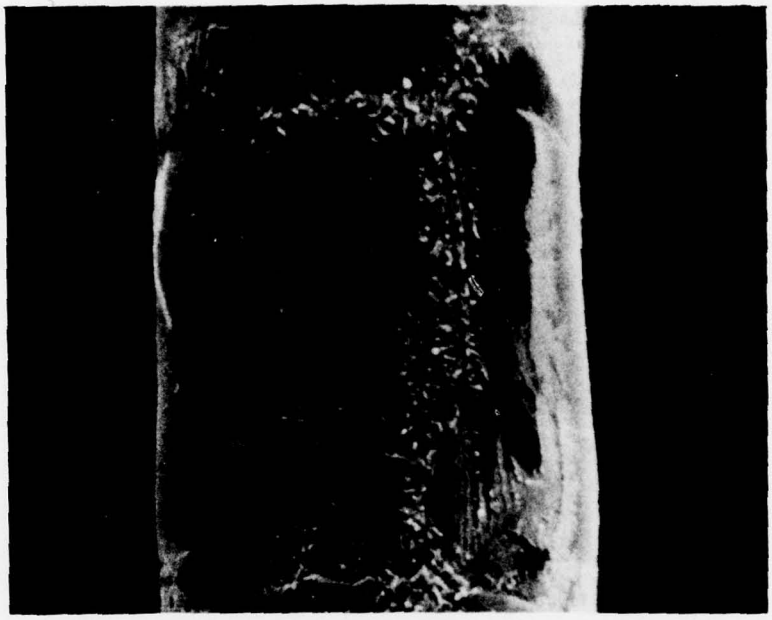

Figure 2 - Vanadium specimen annealed at 1700° C
for 100 hours (S.E.M. 600X)

Figure 3 - Fracture of vanadium specimen annealed at 1700° C for 25 hours (S.E.M. 700X)

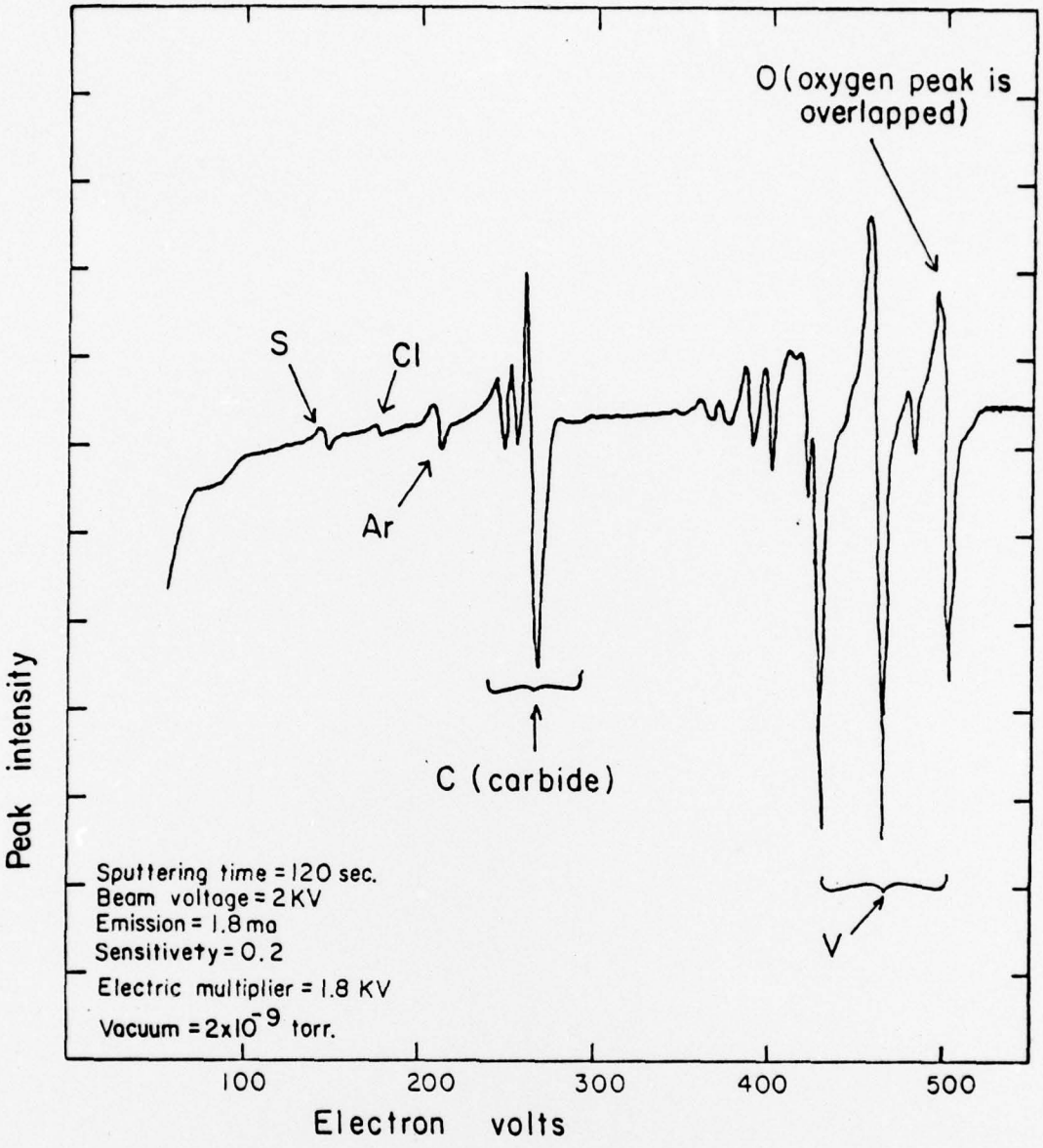

Figure 4 - Reproduction of Auger electron microscopy analysis of embrittled vanadium's surface.

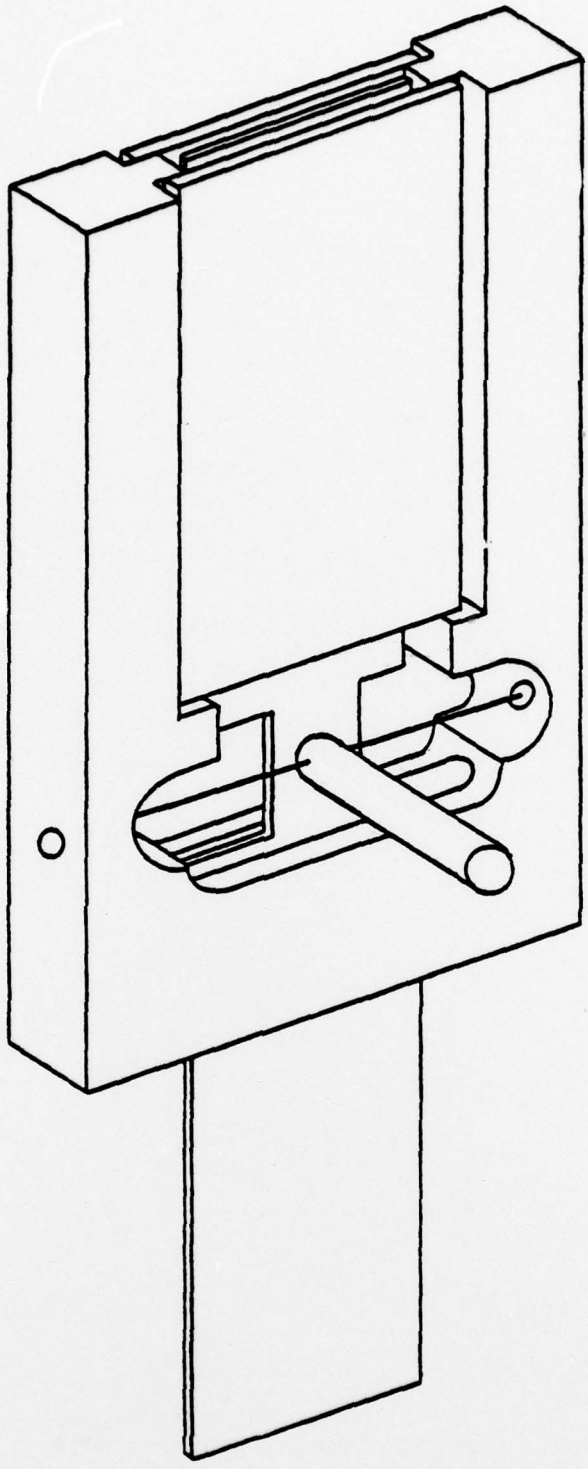

Figure 5 - Capacitance-Torsion balance comprising a horizontal tungsten wire carrying the rotatable plate of the pair of condensers.

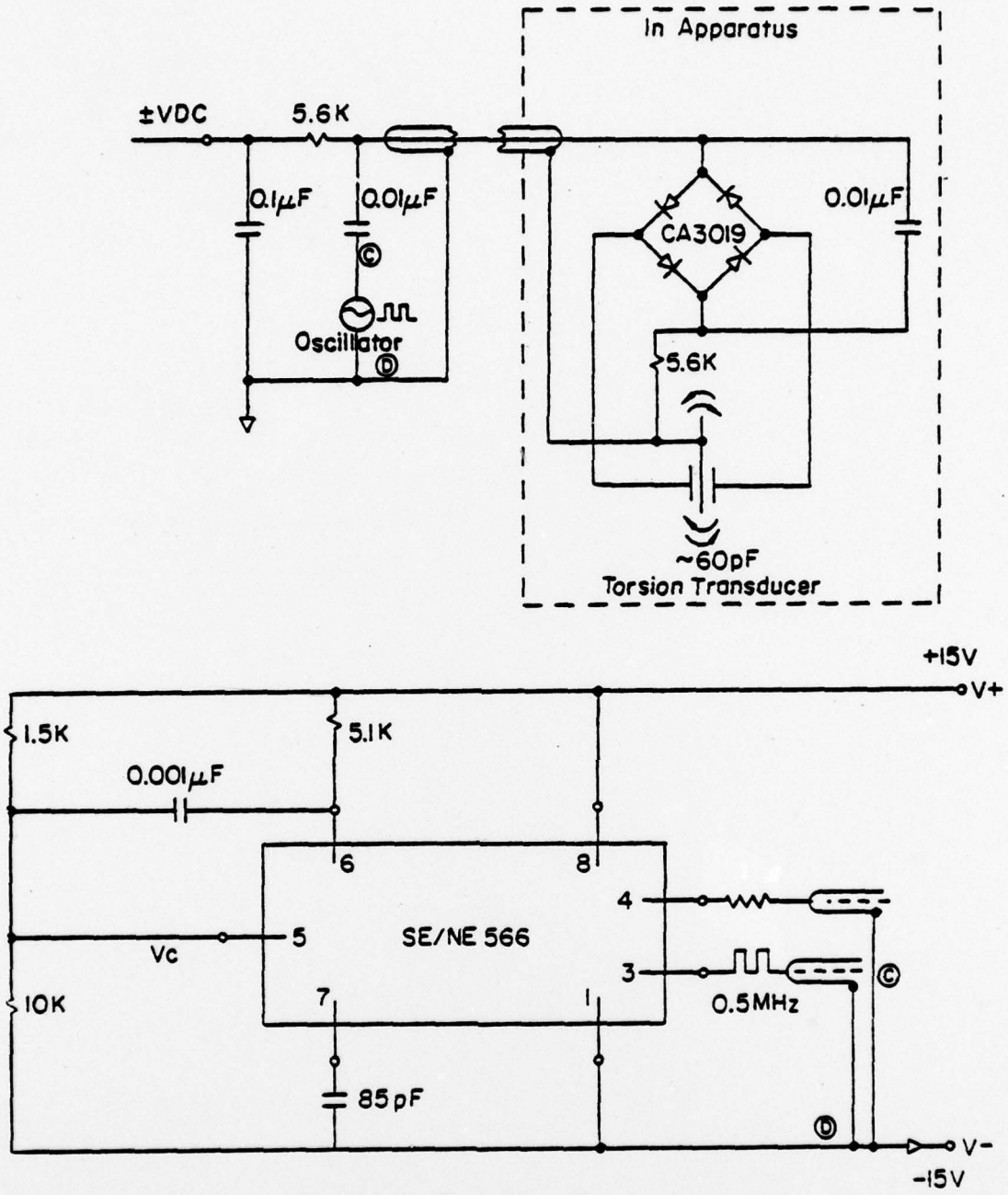

Signetics Function Generator
SE/NE 566

Figure 6

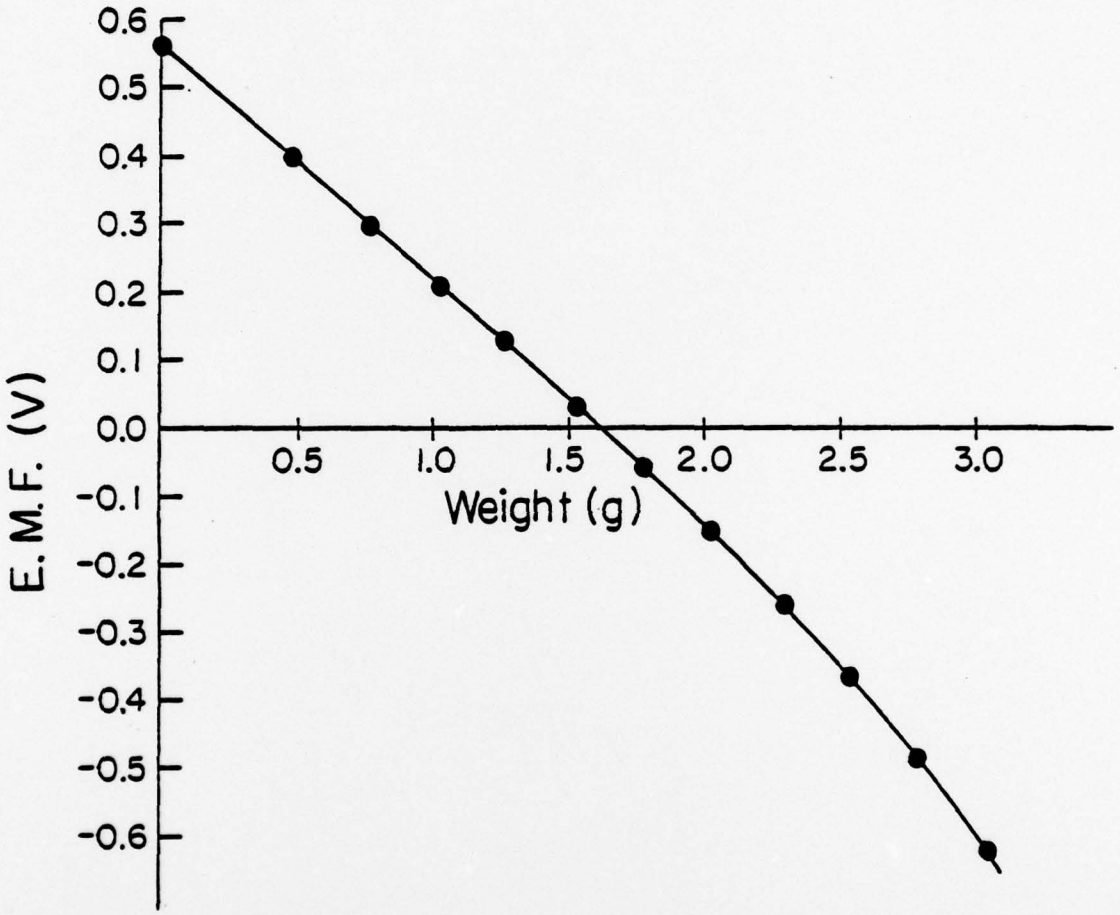

Figure 7 - An example of the relationship between the output voltage and weight applied.

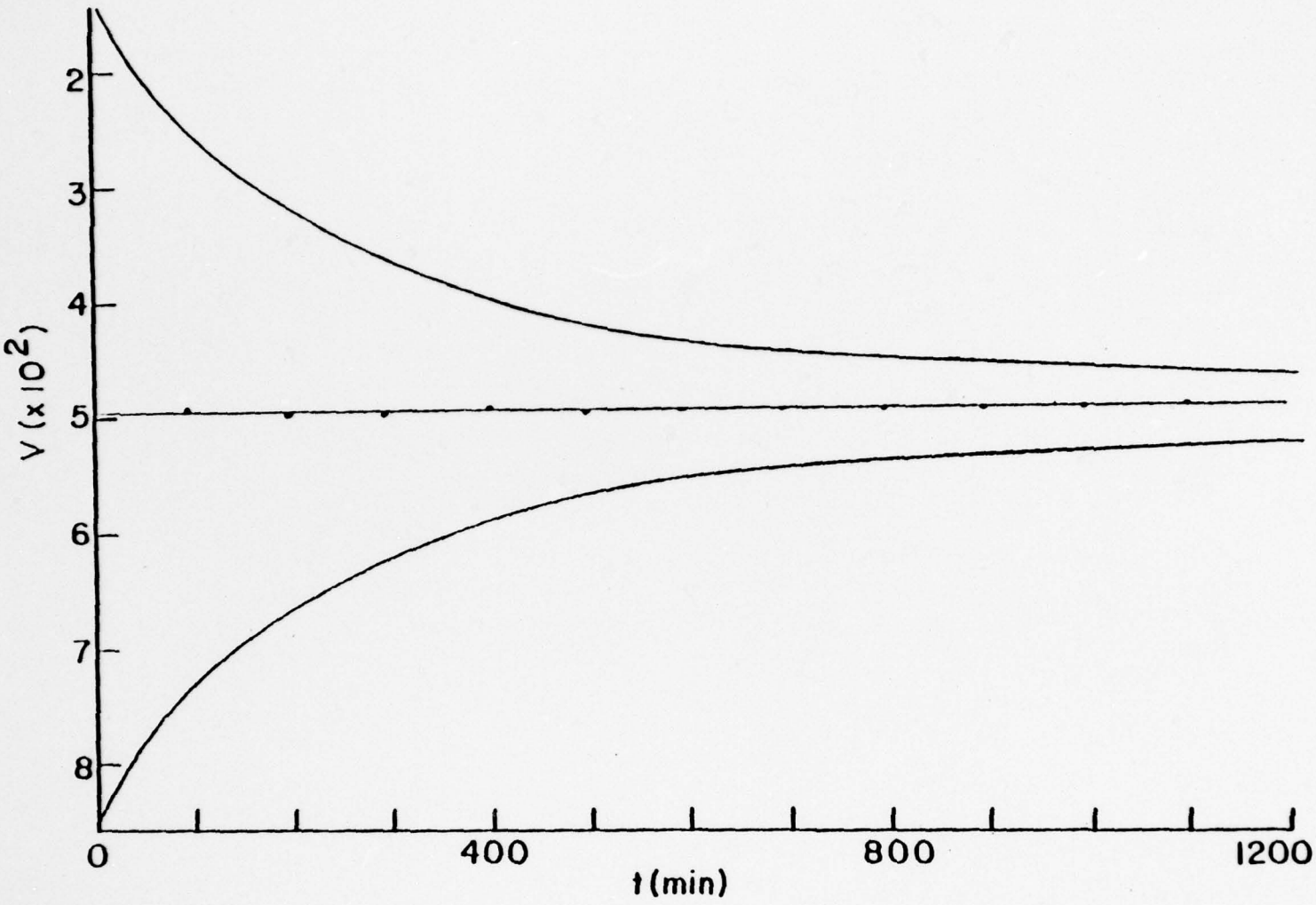

Figure 8 - Volts(V) vs time(t) for copper using S.L.R. technique.

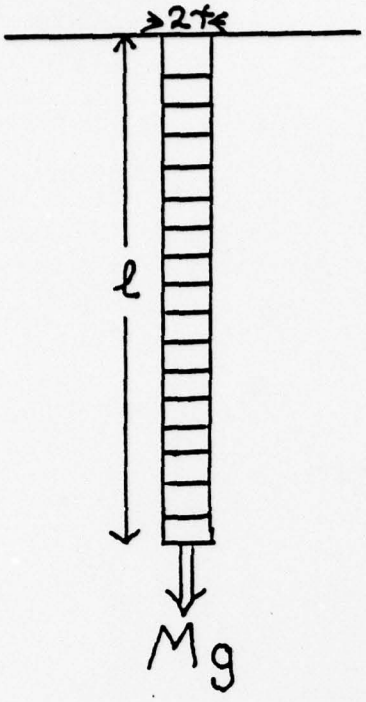

WIRE

Figure 9

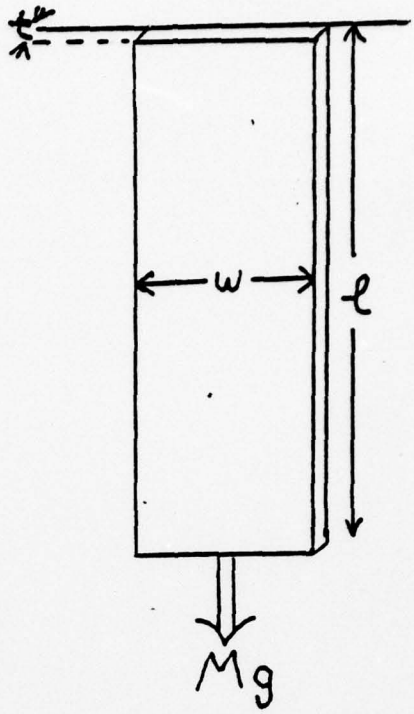

FOIL

Figure 10

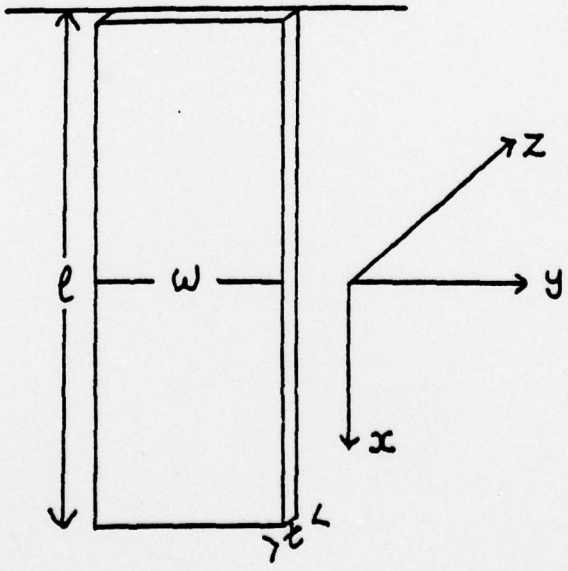

FOIL

Figure 11